



# 1 Retrieving characteristics of IGW parameters with least 2 uncertainties using hodograph method

3 Gopa Dutta, P. Vinay Kumar and Salauddin Mohammad  
4 Vignana Bharathi Institute of Technology, Hyderabad 501301, India.  
5 *Corresponding author:* Gopa Dutta (gopadutta@yahoo.com)

6 **Abstract.** We have analyzed time series of wind velocities measured with high resolution GPS-radiosonde  
7 ascents continuously for 120 h from Hyderabad with an interval of 6 h. Hodograph method has been used to  
8 retrieve the IGW parameters. Background winds are removed from the time series by detrending whereas  
9 polynomials of different orders are removed to get the fluctuations from individual profiles. Butterworth filter is  
10 used to extract monochromatic IGW component. Another filter FIR1 is tried in a similar manner to test the  
11 effects of filters in estimating IGW characteristics. Results reveal that the fluctuation profiles differ with the  
12 change of polynomial orders, but the IGW parameters remain same when Butterworth filter is chosen to extract  
13 the monochromatic wave component. FIR1 filter also produces acceptable results with a broader range. The  
14 direction of wave propagation is confirmed with additional temperature information which needs a large number  
15 of hodographs for statistical significance.

## 16 1 Introduction

17 It is well documented that gravity waves of different scales play an important role in maintaining the large-scale  
18 circulation of the middle atmosphere. A large number of studies have been carried out to characterize these  
19 waves by using different techniques. A very common, established and standard procedure of characterizing  
20 Inertia Gravity Waves (IGW) with frequencies close to Coriolis frequency is by hodograph method (Guest et al.,  
21 2000; Ogino et al., 2006; Niranjana Kumar et al., 2011). Radiosonde data of horizontal winds and temperature  
22 have been extensively used to study these waves (Tsuda et al., 2004; Vincent and Alexander, 2000; Gong et al.,  
23 2008; Chane-Ming et al., 2010, 2014; Murphy et al., 2014; Kramer et al., 2015). Nastrom and VanZandt (1982)  
24 reported good accuracy in gravity wave parameters derived using balloon measurements since balloons have  
25 good aerodynamic responses. In a simulation study Wei and Zhang (2014) have demonstrated that gravity  
26 waves with different frequencies and generated by different sources like jet-imbalance and convection can  
27 coexist together. The popular hodograph method demands the presence of a single coherent wave in the  
28 fluctuation profiles and does not yield good result when a mixture of various frequencies are present. The  
29 gravity wave parameters extracted by hodograph method might also be inaccurate when multiple waves are  
30 present in the data (Eckermann and Hocking, 1989).  
31 Hodograph method is based on linear theory of gravity waves whereas the dynamics of the flow is more  
32 complex and non-linear which introduces some uncertainties in the interpretation. There are several sources of  
33 errors in this method which have been described in Zhang et al., (2004). These authors compared the gravity  
34 wave characteristics obtained using hodograph method with the values derived from 4D output of their  
35 simulation study. A narrow bandwidth filter used by them to extract the fluctuations of a near-monochromatic  
36 wave resulted in large uncertainties in the horizontal wavelength which got reduced for waves with shorter



37 vertical wavelengths. Even the spatial variations of the wave characteristics were found to be large. Moreover,  
38 since the hodographs are quite variable, a large number of hodographs (profiles) are required to get accurate  
39 results of gravity wave parameters with some statistical significance (Hall et al., 1995). This defeats the very  
40 advantage of the hodograph method which is capable of retrieving GW parameters from a single set of vertical  
41 profiles of zonal and meridional winds.

42 The present paper attempts to overcome the inconsistency of hodograph method in delineating the  
43 characteristics of IGW from velocity fluctuations obtained with radiosonde measurements.

## 44 **2 Experiment and Data**

45 An intensive campaign with high resolution (i-Met, USA) GPS–radiosonde flights was carried out from the  
46 campus of India Meteorological Department (IMD), Hyderabad (17.4 °N, 78.5 °E) with four flights a day at an  
47 interval of 6 h for 5 consecutive days (20 flights) between 30 April and 4 May, 2012 to study the characteristics  
48 of IGW. The timings of the flights were 05:30, 11:30, 17:30 and 23:30 LT. The accuracy of wind and  
49 temperature measurements provided by the manufacturer is  $\pm 1 \text{ ms}^{-1}$  and  $\pm 0.2 \text{ K}$  respectively. There was one  
50 data gap at 11:30 LT on 4 May, 2012 which was linearly interpolated to get continuous time series of wind  
51 velocities. High resolution ( $\sim 4 - 10 \text{ m}$ ) wind data obtained directly from balloon flights were first sorted in  
52 ascending order of height since the balloons occasionally drift downwards by a few meters. Wind profiles were  
53 visually inspected for outliers and such outliers, if any, were removed. The gaps were filled up by linear  
54 interpolations. The wind profiles were then interpolated vertically to have a constant height resolution of 50 m.  
55 This method is useful to smooth the profiles and to maintain a good resolution in height.

## 56 **3 Analysis and Discussion**

57 Experiments were carried out for five days with a view to getting continuous horizontal wind velocities for 120  
58 h with a regular interval of 6 h keeping in mind that the IGW period over the site is  $\sim 40 \text{ h}$ . The continuous zonal  
59 and meridional wind datasets are detrended (linear trend removed) to obtain time series of fluctuations. A third  
60 order Butterworth filter with a band-pass between 36 and 44 h is applied to the wind perturbations to retrieve the  
61 IGW fluctuations with zero phase distortion. The sufficiently wide band of the time filter is helpful to reduce the  
62 Doppler shift of IGW frequency (Niranjan Kumar et al., 2011). Ehard et al., (2015) also recommended the usage  
63 of Butterworth filter in extracting gravity waves over a wide range of periods from temperature perturbations  
64 measured by lidar. The filtered horizontal winds at particular heights are depicted in Fig. 1a – 1d which show  
65 the presence of IGW with a period of  $\sim 40 \text{ h}$ . FFT analyses carried out with filtered wind data also reveal the  
66 presence of a clear monochromatic wave of the same period (Fig. 1e – 1h) which satisfies the requirement of  
67 hodograph method.

68 Hodographs plotted with this time-wise filtered zonal and meridional wind perturbations ( $u'$ ,  $v'$ ) are quite noisy  
69 and it is difficult to identify proper closings. The fluctuation profiles are, therefore, further band-pass filtered  
70 with a cut-off at 1.5 – 4 km which produced proper elliptic hodographs. The number of proper hodographs  
71 obtained from 20 pairs of vertical profiles of  $u'$  and  $v'$  are 124. A few IGW parameters have been extracted  
72 assuming linear dispersion relations (Cho, 1995; Tsuda et al., 1994). The intrinsic wave frequency ( $\omega$ ) is  
73 calculated from the ratio of minor to major axes of the ellipse.



74 
$$\frac{v'}{w'} = -i \left( \frac{f}{\omega} \right), \quad (1)$$

75 where  $f$  is the inertial frequency and  $v', u'$  are the meridional and zonal wind fluctuations respectively.  $f$  is  
76 computed as

77 
$$f = \frac{\sin \varphi}{1/2 \text{ day}} \quad (2)$$

78 where  $\varphi$  is the latitude of the place. The horizontal wave number  $k$  is found using the relation

79 
$$k = m\omega/N \quad (3)$$

80  $N$  being the Brunt – Väisälä frequency and  $m$  is vertical wave number.

81 Intrinsic periods of IGW obtained from hodographs range between 20 – 28 h. The vertical and horizontal  
82 wavelengths inferred from the hodographs are between 2.0 to 2.8 km and between 493 – 846 km respectively.  
83 The direction of horizontal wave propagation is parallel to the major axis of the ellipse which is uncertain by  
84 180°. This uncertainty can be removed with the help of additional temperature information. Temperature  
85 perturbation profiles are obtained by removing 5<sup>th</sup> order polynomial fits from the simultaneous temperature  
86 profiles and filtering them height-wise with a band-pass Butterworth filter between 1.5 and 4 km. Hodographs  
87 of  $u' - v'$  and  $u' - t'$  are capable of deciding the final directions of propagation of the wave (Hu et al., 2002). The  
88 unambiguous direction of propagation of IGW is observed to be south-east (62%) in this analysis.

89 Next we chose a different filter FIR1 of order 6 to test the effect of filtering on hodograph method since the  
90 vertical wavelength and intrinsic frequency are reported to be highly vulnerable to the filter used (Zhang et al.,  
91 2004). We followed the same procedure to delineate the IGW parameters as described before using Butterworth  
92 filter. The detrended and time-wise filtered horizontal wind profiles at a few heights and the corresponding FFT  
93 peaks are illustrated in Fig. 2a – 2d and 2e – 2h respectively. Both the time variation of wind fluctuations and  
94 the FFT peaks do not show distinct IGW periods. The frequency responses of Butterworth filter of 3<sup>rd</sup> order and  
95 FIR1 of 6<sup>th</sup> order are shown in Fig. 3. The Butterworth filter shows a sharp cut-off and also has the advantage of  
96 producing good result with a much lower filter order than the corresponding FIR1 filter. A few hodographs  
97 plotted with horizontal wind perturbations using both the filters are displayed in Fig. 4a – 4d. The IGW  
98 parameters derived from these hodographs are listed in Table 1. The ranges of horizontal wavelength, vertical  
99 wavelength and intrinsic period are observed to be broader using FIR1 filter compared to those obtained using  
100 Butterworth filter.

101 Hodographs are generally plotted with the fluctuations derived from data of individual sounding by removing  
102 polynomials of 1<sup>st</sup> or 2<sup>nd</sup> order. We treated the measured vertical profiles of zonal and meridional winds as  
103 single individual set (not time series) and approximated the backgrounds by polynomials of different (2 to 9)  
104 orders. Fig.5 depicts the different fits and the corresponding wind profiles. The fluctuation profiles obtained by  
105 removing polynomials of 4, 5 and 6 orders show close agreements whereas appreciable differences could be  
106 noticed for others (figure not shown). These profiles are then filtered with a 3<sup>rd</sup> order Butterworth filter height-  
107 wise to retain IGW oscillations with short vertical wavelengths (1.5 – 4 km). IGW parameters obtained from the  
108 hodographs plotted with these fluctuations match extremely well with those delineated from the previous  
109 computation where the background was removed from the time series by detrending and filtering was done both  
110 time-wise (36 – 44 h) and height-wise (1.5 – 4 km).



111 The individual profiles of winds and temperature are then analyzed in a similar manner using FIR1 filter with  
112 height instead of Butterworth filter. The perturbation profiles (after removing backgrounds with different orders)  
113 and the filtered fluctuation profiles using both Butterworth and FIR1 filters are shown in Fig. 6a – 6c and 6d –  
114 6f for both the wind components, respectively. It is clearly observed that the Butterworth filter can extract the  
115 monochromatic IGW fluctuations very efficiently. The retrieved IGW parameters retain same numerical values  
116 (except after decimal points) irrespective of the background removals. Results obtained with FIR1 filter also  
117 belong to the same range but with a broader band which is illustrated in Table 2 for different orders. The  
118 direction of propagation of IGW inferred from different ways of computation is unambiguously south-east. This  
119 demands a large number of hodographs to finalize the direction with some statistical significance.

#### 120 **4 Summary**

121 Balloon borne experiments have been conducted for five days with an interval of 6 h to characterize IGW using  
122 hodograph method. The method is helpful in identifying low-frequency IGW but suffers from several  
123 uncertainties. We have utilized the time series of wind fluctuations to extract IGW component by filtering and  
124 confirmed it with spectral analysis. Results obtained by using Butterworth and FIR1 filters are compared. A  
125 band-pass Butterworth filter with a sharp cut-off is found to isolate the monochromatic IGW component very  
126 efficiently. Backgrounds of individual wind profiles have been approximated with polynomials of different  
127 orders when the perturbation profiles show reasonable differences. The differences are observed to get reduced  
128 when Butterworth filter is used to isolate the IGW components, whereas differences still persist with FIR1 filter.  
129 IGW parameters delineated from the corresponding hodographs using the former filter agree extremely well for  
130 different order polynomial removal. Results obtained with FIR1 filter also show reasonable agreement but with  
131 a broader range. Filtering appears to be of great importance in removing uncertainties of hodograph method.  
132 The unambiguous direction of wave propagation can be ascertained using additional and simultaneous  
133 temperature information but a large number of hodographs are needed to confirm it with statistical significance.

#### 134 **Acknowledgements**

135 Authors are grateful to Indian Space Research Organization (ISRO), Government of India, for providing  
136 financial assistance to run the project under its Climate And Weather of Sun–Earth System (CAWSES–II)  
137 program. The authors wish to thank India Meteorological Department (IMD), Hyderabad, for their active  
138 support to conduct the balloon experiments from their campus. The authors also thank the college management  
139 for kind encouragement. Data is available at Vignana Bharathi Institute of Technology, Hyderabad, India. We  
140 would like to thank Dr. K Kishore Kumar, Space Physics Laboratory (SPL) for his valuable discussions.

#### 141 **References**

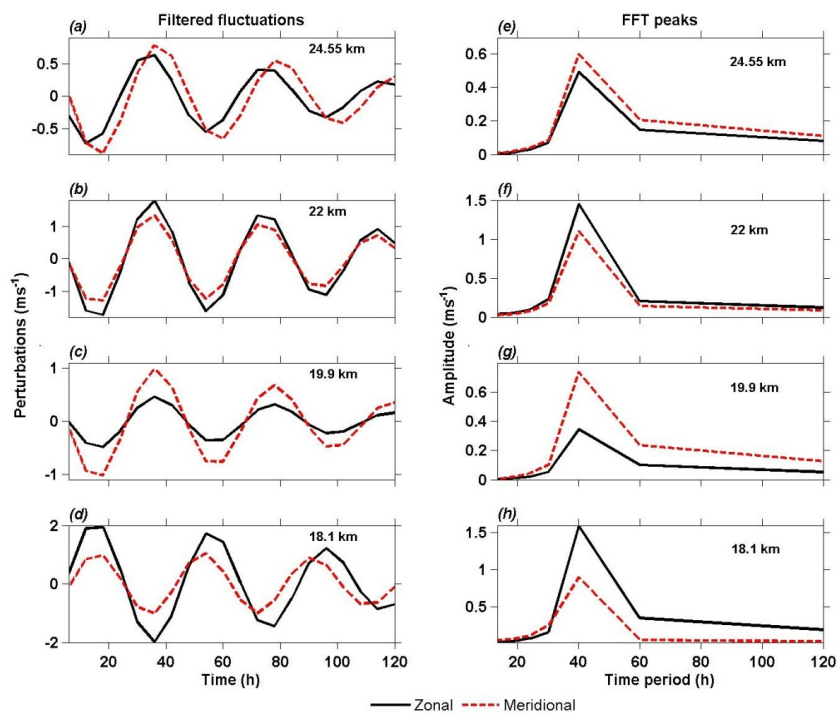
- 142 Chane-Ming, F., Chen, Z., and Roux, F.: Analysis of gravity-waves produced by intense tropical cyclones,  
143 *Annales Geophys.*, 28, 531-547, 2010.
- 144 Chane-Ming, F., Ibrahim, C., Barthe, C., Jolivet, S., Keckhut, P., Liou, Y.-A., and Kuleshov, Y.: Observation  
145 and a numerical study of gravity waves during tropical cyclone Ivan (2008), *Atmos. Chem. and Phys.*, 14, 641–  
146 658, 2014, doi:10.5194/acp-14-641-2014, 2014.



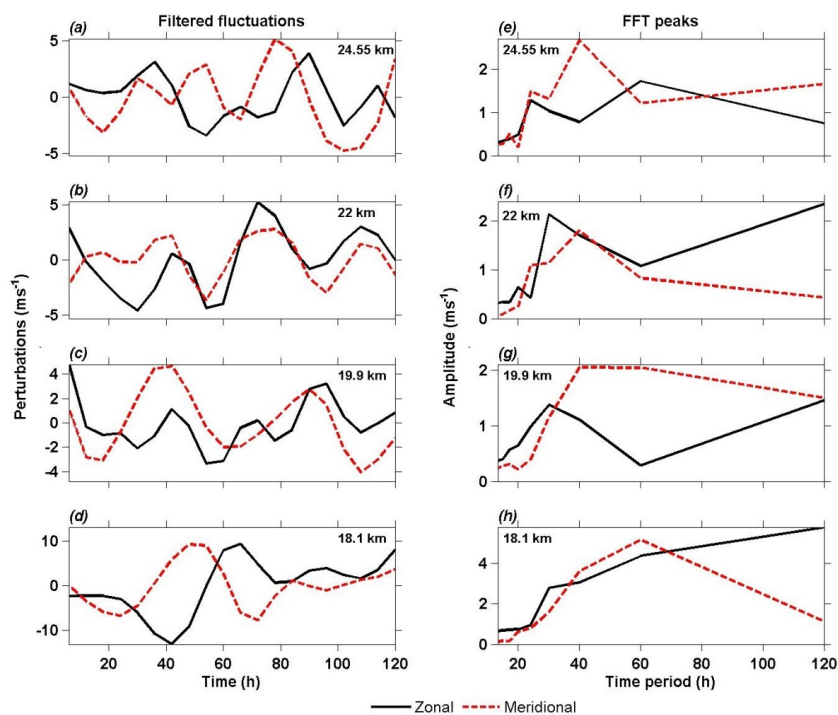
- 147 Cho, J. Y. N.: Inertio-gravity wave parameter estimation from cross-spectral analysis, *J. Geophys. Res.*, 100,  
148 D9, 18727-18737, 1995.
- 149 Eckermann, S. D., and Hocking, W. K.: Effect of superposition on measurements of atmospheric gravity waves:  
150 a cautionary note and some reinterpretations, *J. Geophys. Res.*, 94, 6333-6339, 1989.
- 151 Ehard, B., Kaifler, B., Kaifler, N., and Rapp, M.: Evaluation of methods for gravity wave extraction from  
152 middle-atmospheric lidar temperature measurements, *Atmos. Meas. Tech.*, 8, 46454655,  
153 doi:10.5194/amt846452015, 2015.
- 154 Gong, J., Geller, M. A., and Wang, L.: Source spectra information derived from U.S high-resolution radiosonde  
155 data, *J. Geophys. Res.*, 113, D10106, doi:10.1029/2007JD009252, 2008.
- 156 Guest, F., Reeder, M. J., Marks, C. J., and Karoly, D. J.: Inertia-Gravity wave observed in the lower stratosphere  
157 over Macquarie Island, *J. Atmos. Sci.*, 57, 737-752, 2000.
- 158 Hall, G. E., Meek, C. E., and Manson, A. H.: Hodograph analysis of mesopause region winds observed by three  
159 MF radars in the Canadian prairies, *J. Geophys. Res.*, 100, 7411-7421, 1995.
- 160 Hu, X., Liu, A. Z., Gardner, C. S., and Swenson, G. R.: Characteristics of quasi-monochromatic gravity waves  
161 observed with Na lidar in the mesopause region at Starfire Optical Range, NM, *Geophys. Res. Lett.*, 29 (24),  
162 doi:10.1029/2002GL014975, 2002.
- 163 Kramer, R., Wüst, S., Schmidt, C., and Bittner, M.: Gravity wave characteristics in the middle atmosphere  
164 during the CESAR campaign at palma de Mallorca in 2011/2012: Impact of extratropical cyclones and cold  
165 fronts, *J. Atmos. Sol. Terr. Phys.*, 128, 8-23doi:10.1016/j.jastp.2015.03.001, 2015.
- 166 Murphy, D. J., Alexander, S. P., Klekociuk, A. R., Love, P. T., and Vincent, R. A.: Radiosonde observations of  
167 gravity waves in the lower stratosphere over Davis, Antarctica, *J. Geophys. Res.*, 119, 11,973–11,996,  
168 10.1002/2014 JD022448, 2014.
- 169 Niranjana Kumar, K., Ramkumar, T. K., and Krishnaiah, M.: MST radar observation of inertial-gravity waves  
170 generated from tropical cyclones, *J. Atmos. Sol. Terr. Phys.*, 73, 1890-1906, doi:10.1016/j.jastp.2011.04.026,  
171 2011.
- 172 Nastrom, G. D., and VanZandt, T. E.: An analytical study of nonlinear responses of rising balloons in horizontal  
173 winds, *J. Appl. Meteorol.*, 21, 413-419, 1982.
- 174 Ogino, S. Y., Sato, K., Yamanaka, M. D., and Watanabe, A.: Lower stratospheric and upper-tropospheric  
175 disturbances observed by radiosondes over Thailand during January, 2000, *J. Atmos. Sci.*, 63, 3437-3447, 2006.
- 176 Tsuda, T., Murayama, Y., Wiryosumarto, H., Harijono, S. W. B., and Kato, S.: Radiosonde observations of  
177 equatorial atmospheric dynamics over Indonesia, 2. Characteristics of gravity waves. *J. Geophys. Res.*, 99,  
178 10507-10516. 1994.
- 179 Tsuda, T., Ratnam, M. V., May, P. T., Alexander, M. J., Vincent, R. A., and MacKinnon, A.: Characteristics of  
180 gravity waves with short vertical wavelengths observed with radiosonde and GPS occultation during DAWEX  
181 (Darwin Area Wave Experiment), *J. Geophys. Res.*, 109, D20S03, doi:10.1029/2004JD004946, 2004.
- 182 Vincent, R. A., and Alexander, M. J.: Gravity wave in the tropical lower stratosphere: An observational study of  
183 seasonal and inter-annual variability, *J. Geophys. Res.*, 105, 17971-17982, 2000.
- 184 Wei, J., and Zhang, F.: Mesoscale gravity waves in moist baroclinic jet-front systems. *J. Atmos. Sci.*, 71, 929–  
185 952, doi:10.1175/JASD130171.1, 2014.



186 Zhang, F., Wang, S., and Plougonven, R.: Uncertainties in using the hodograph method to retrieve gravity wave  
187 characteristics from individual soundings, *Geophys. Res. Lett.*, 31, L11110, doi:10.1029/2004GL019841, 2004.

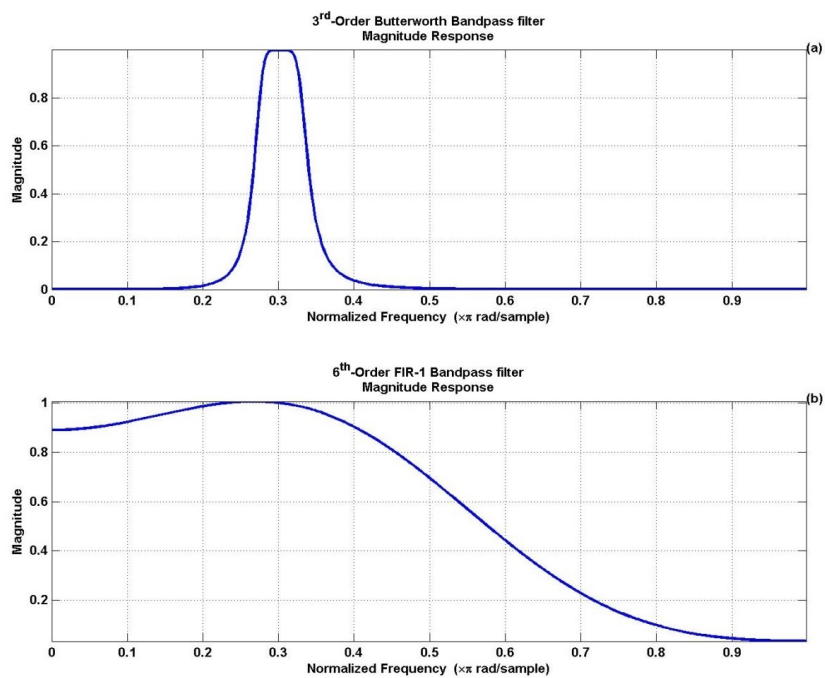


188  
189 **Figure 1.** Time series of filtered (Butterworth filter) fluctuations ( $\text{ms}^{-1}$ ) of zonal and meridional winds (a – d)  
190 and corresponding FFT spectra (e – f) at a few heights.



191  
192

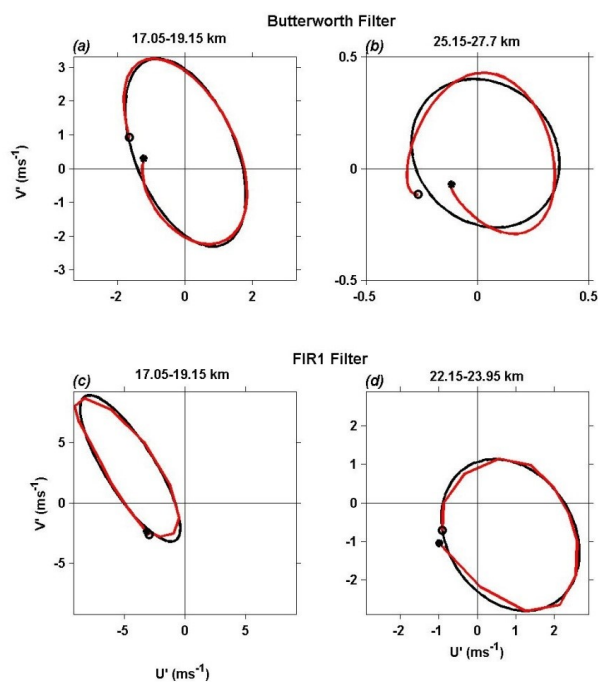
Figure 2. Same as in Figure 1 but with FIR1 filter.



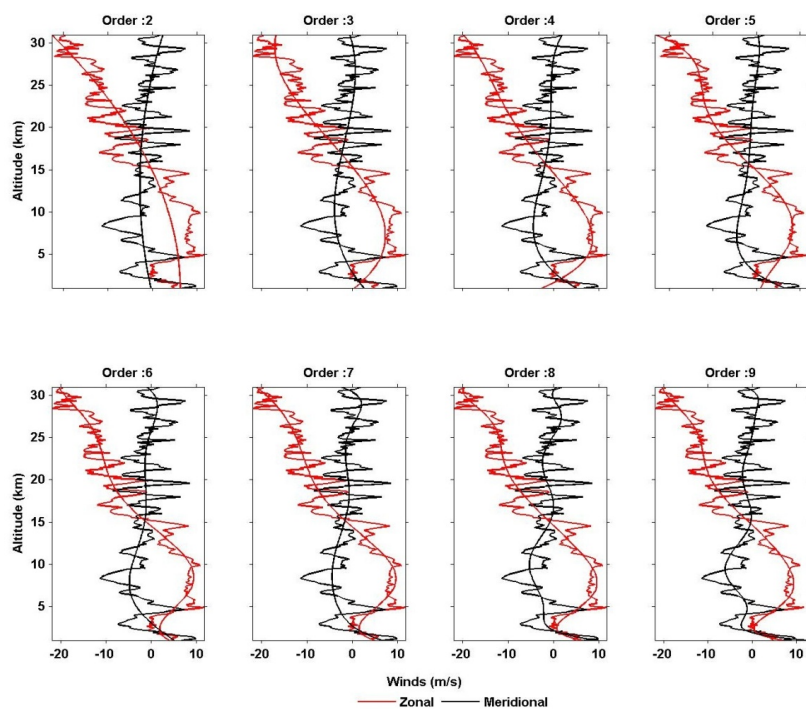
193  
194

Figure 3. The filter responses of Butterworth (a) and FIR 1(b) filters.



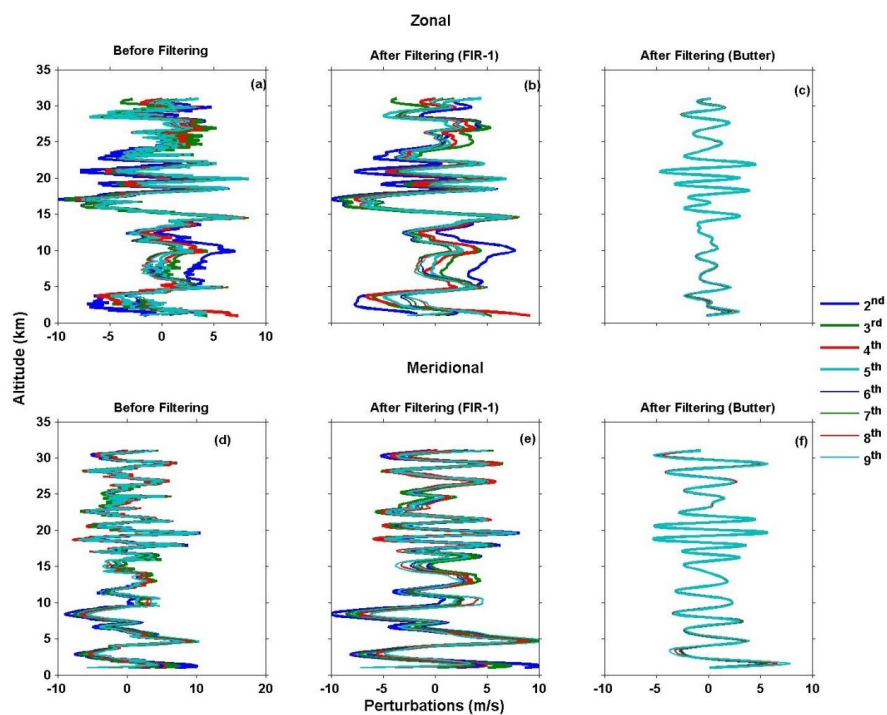


195  
196 **Figure 4.** Hodographs of horizontal wind fluctuations ( $\text{ms}^{-1}$ ) obtained using Butterworth (a, b) and FIR1 (c, d)  
197 filters. An open circle and a solid circle in each hodograph indicate the lowest and highest altitudes,  
198 respectively. The thin curves represent the elliptical fits.



199  
200

**Figure 5.** Profiles of zonal and meridional winds ( $\text{ms}^{-1}$ ) and their fits with different orders.



201  
202 **Figure 6. Upper panel:** Vertical profiles of zonal wind fluctuations ( $\text{ms}^{-1}$ ) after approximating the backgrounds  
203 with different order ( $2^{\text{nd}} - 9^{\text{th}}$ ) polynomials (a) and filtering height-wise with Butterworth filter (b) and FIR1  
204 filter (c). **Lower panel:** Same as upper panel but for meridional wind fluctuations.

205



206 **Table 1:** Comparison of IGW parameters using detrended time series fluctuations and obtained with different  
207 filters

Parameters	Butterworth filter	FIR1 filter
Horizontal wavelength (km)	493 – 836	227 – 800
Vertical wavelength (km)	2.0 – 2.8	1.5 – 3.5
Intrinsic Period (h)	20 – 28	10 – 30
Ratio of minor to major axis	0.44 – 0.76	0.35 – 0.87
Direction of propagation	South-East (62%)	South-East (63%)

208



209 **Table 2:** Comparison of IGW parameters using individual set of wind fluctuation profiles by removing the  
 210 backgrounds with different order polynomial fits and using both the filters.

Parameters		Horizontal wavelength (km)	Vertical wavelength (km)	Intrinsic Period (h)	Ratio of minor to major axis	Direction of propagation
Filter	Order number					
Butterworth	2 to 9	388-770	2.0-2.6	16.25	0.34-0.71	South-East (52%)
	2	300-722	1.7-4	15.23	0.34-0.71	South-East (63%)
FIR1	3	426-663	1.7-4	17.3-23.9	0.32-0.71	South-East (65%)
	4	371-683	1.7-3.2	15.8-23.5	0.32-0.71	South-East (64%)
	5	250-850	1.8-3.1	16-25	0.32-0.7	South-East (60%)
	6	332-712	1.7-4	15.8-24.7	0.3-0.69	South-East (66%)
	7	403-711	1.7-4	16.1-25.4	0.3-0.69	South-East (65%)
	8	330-685	1.8-3.1	16-25	0.32-0.68	South-East (63%)
	9	322-577	1.7-4	16.2-25	0.31-0.68	South-East (66%)

211